Light-Induced Charge Separation at Sensitized Sol−Gel Processed Semiconductors

Jeremy M. Stipkala,† Felix N. Castellano,† Todd A. Heimer,† Craig A. Kelly,† Kenneth J. T. Livi,‡ and Gerald J. Meyer*,†

Department of Chemistry and Department of Earth and Planetary Science, Johns Hopkins University, Baltimore, Maryland 21218

Received May 7, 1997. Revised Manuscript Received July 18, 1997⊗

The photophysical properties of molecular sensitizers incorporated within sol−gel processed wide-bandgap semiconductors are reviewed. Excited-state interfacial electron transfer in sensitized colloids and colloidal films provides a basis for the conversion of photons into potential energy. Sol−gel processed materials with high transparency in the visible region allow charge separation and recombination processes to be quantified spectroscopically. The yields and dynamics of these processes are reviewed for a wide variety of sensitizer−semiconductor assemblies. Implications for solar energy conversion and other molecular device applications are discussed.

I. Introduction and Background

A. Introduction. Sol−gel chemistry provides a convenient approach for the preparation of wide-band-gap semiconductors with distinct advantages over other semiconductor processing routes.[1] These include the ability to tailor surface and bulk properties to form metastable phases under ambient conditions (such as anatase TiO_2), low-temperature processing, and the ability to cast the materials in virtually any shape or form. The mild processing conditions allow one to spatially arrange and isolate a variety of molecular components within metal oxide semiconductors, such as TiO_2, ZnO, and SnO_2, and provides the basis for new classes of molecular level devices.[2] Further, semiconductor materials with high optical transparency can be prepared that permit the photophysical properties of molecular excited states to be spectroscopically and electrochemically probed in a manner that was not previously possible.[3] Optical studies through the solution-to-gel transition allow the supramolecular nature of extended solids to be systematically explored on a molecular level.[4] These are the subject of this review article.

Detailed reviews of excited-state processes within sol−gel processed insulators have recently appeared in the literature.[4] However, this contribution appears to be the first review of molecular excited states integrated into sol−gel processed semiconductor materials. As will be discussed in detail below, the inherent electronic nature of semiconductor metal oxides can directly interact with molecular excited states in a manner not energetically possible with insulators.[3] More specifically, an excited sensitizer, S^*, may transfer an electron to the semiconductor forming a charge separated pair (eq I). For artificial photosynthetic applications, the importance of this charge-separation process is that it provides a molecular basis for the conversion of photons into potential energy.[5] If the interfacial charge-separated pair has a sufficiently long lifetime, it may undergo subsequent bimolecular redox processes forming useful chemical fuels, such as hydrogen and oxygen. For these type of applications, it is desirable to prevent the energy-wasting charge-recombination process that yield ground-state products (eq II). A fundamental goal, therefore, is to form interfacial charge separated states that have long lifetimes.[5]

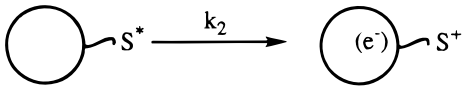

(I)

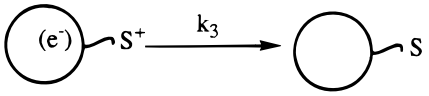

(II)

A particular advantage of interfacial charge-separated states at semiconductor materials is that the injected electron can be collected as an electrical response.[6−11] This forms the basis for new applications that exploit both the electronic and optical properties of the sensitized materials, such as charge storage, displays, chemical sensing, and optical switching.[2] To date, the most promising applications have been in the direct conversion of light into electricity with sensitized nanocrystalline semiconductor films.[6] This science has roots in sensitization studies of single crystal electrodes from the early 1970s.[7−10] The nanocrystalline materials prepared through sol−gel routes display interesting optical and electronic behavior that cannot be rationalized by traditional Schottky junction models and represent the basis for the rapidly growing area of nanostructured photoelectrochemistry where sol−gel science continues to play a key role.[11]

The outlay of this review is as follows. First as background, the sol−gel chemistry of metal oxide materials and potential applications of molecular excited states incorporated within them are briefly presented. This is followed by a literature review of dye sensitized sol−gel processed semiconductor colloidal solutions and colloidal films. The conclusion summarizes these findings and suggests new directions for future research.

† Department of Chemistry.
‡ Department of Earth and Planetary Science.
⊗ Abstract published in *Advance ACS Abstracts,* September 1, 1997.

S0897-4756(97)00317-7 CCC: $14.00

B. Sol−Gel Materials. The sol−gel process involves the hydrolysis (III) and condensation (IV) of metal

$$Ti(OR)_n + H_2O \rightarrow Ti(OR)_{n-1}(OH) + ROH \quad (III)$$

$$Ti(OR)_n + Ti(OR)_{n-1}(OH) \rightarrow Ti_2O(OR)_{2n-2} + ROH \quad (IV)$$

alkoxides to form macromolecular metal oxide networks. In general, the chemistry is far more complex than that shown in Reactions III and IV. For example, the structure and chemical nature of many metal alkoxides remains unknown.[12] These reactions have been studied extensively for the formation of SiO_2.[1] Unfortunately, the sol−gel chemistry of transition metal and other main group metal alkoxides is far less well developed.[12]

Despite this, sol−gel routes to a wide variety of metal oxide materials are available in the literature. Some important observations that have emerged from studies of transition-metal sol−gel chemistry have recently been discussed by Sanchez and Livage.[12] A general "rule of thumb" is that the relative rates for hydrolysis and condensation reactions dictate the physical and chemical nature of the products. Fast hydrolysis followed by slow condensation rates generally lead to the formation of polymeric gels, while fast hydrolysis and fast condensation often yield colloidal gels or gelatinous precipitates. In contrast, slow hydrolysis and condensation reactions leads to the production of colloidal solutions. The rates of hydrolysis and condensation can be systematically controlled with pH, electrolyte, metal alkoxide precursors, temperature, solvent, and hydrolysis ratio.[1]

While the details of the sol−gel chemistry go beyond the scope of this review, suffice it to say that a wide variety of metal oxide materials can be prepared that are ideal for molecular photonic applications.[1,12] Many of these materials have been known for decades. For materials of most relevance to this review, a brief discussion of the preparation and characterization is worthwhile.

1. Colloidal Solutions. Moser and Grätzel have developed a colloidal TiO_2 preparation from the sol−gel processing of $TiCl_4$.[13] $TiCl_4$ (5 g) was added slowly to water (200 mL) at 0 °C, and the resulting solution was dialyzed to pH 3. UV- purified poly(vinyl alcohol) was used to stabilize the sol above pH 3. Roughly spherical particles of 50 Å consisting of anatase and some amorphous TiO_2 were produced.[13] The procedure of Micic uses 2.2 mL of $TiCl_4$ cooled to −20 °C added dropwise to cold water (0 °C) and then dialyzed with deionized water.[14] The TiO_2 particles were approximately 4−7 nm in diameter (Figure 1) and colloidal solutions display negligible absorption or light scattering at wavelengths longer than 400 nm. Titration with peroxide was used to calculate the TiO_2 concentrations. Preparations of TiO_2 colloidal sols from titanium tetraalkoxides are also well documented.[15,16]

A sol−gel route to 55 Å wurtzite ZnO particles was reported by Spanhel and Anderson.[17] As the colloids aged, the authors observed a sharpening of X-ray diffraction peaks, indicating an increasing degree of crystallinity; these observations are suggestive of Ostwald ripening.[17]

Commercial SnO_2 colloidal dispersions (Johnson Matthey), often used in sensitization experiments, are available. These consist of 15−18% cassiterite SnO_2 colloids, produced in a proprietary procedure, suspended in pH 9−10.5 water with a 0.3−0.5% NH_4^+ or K^+ counterion concentration.[18]

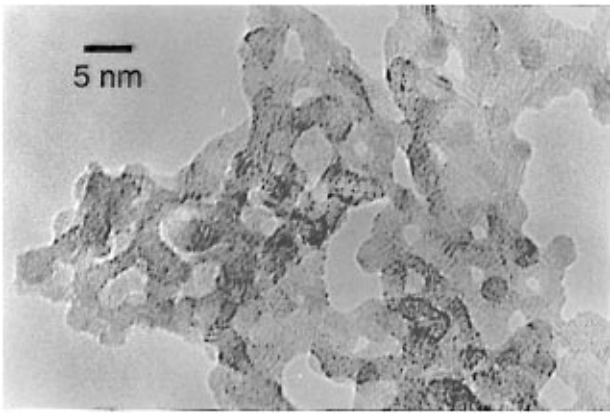

Figure 1. Transmission electron micrograph of colloidal TiO_2 particles prepared from $TiCl_4$.

2. Nanocrystalline Films. Several routes to porous nanocrystalline TiO_2 films exist.[19−22] Early reports indicated use of the "fractal" preparation, so-called because of the geometry of the resulting colloidal film. Fractal TiO_2 films were made in a manner similar to high-temperature hydrolysis procedures.[19] In a typical preparation, $TiCl_4$ (21 mmol) was dissolved in absolute ethanol (10 mL) and diluted with methanol to a Ti concentration of 25 or 50 mg/mL. A titanium foil or a fluorine-doped SnO_2 (FTO) electrode is dipped into this solution, coating the substrate with titania species. This layer is then hydrolyzed in a humid chamber at room temperature for 30 min, followed by sintering in air at 450 °C. The coating, hydrolysis, sintering step can be repeated to add several coats of TiO_2 to the substrate. After the final coat of TiO_2 was deposited, the electrode was sintered one final time at 550 °C under an Ar atmosphere, creating a white, high surface area film.

Commercially available Degussa P-25 TiO_2 is made via flame hydrolysis of $TiCl_4$, producing a highly dispersed powder with an average diameter of 21 nm and a specific surface area of 50 m^2/g.[20] This synthesis is obviously not a sol−gel process; however, since fundamental studies have been conducted in the area of dye sensitization of particulate semiconductors with Degussa P-25, we have included some relevant results in our discussion.

A key step forward was the preparation of transparent colloidal anatase films.[6,21] A preparation that is now widely used is as follows: 50 mL of Ti(*i*-OPr)$_4$ was added over 10 minutes to a stirred solution of 300 mL of deionized water and 2.1 mL of 70% nitric acid in a flask open to the air. A flaky white precipitate formed immediately upon addition of the alkoxide. The mixture was then heated to reflux with continued stirring for 8 h. During this time the precipitate dissolved and the solution became nearly transparent. The solution was then cooled, and the final volume was adjusted with water to achieve a concentration of 150−170 g of TiO_2/L (based on complete reaction of the initial Ti(*i*-OPr)$_4$). Approximately 25 mL of the 150 g/L TiO_2 solution was placed in an acid digestion bomb and heated to 200 °C overnight. After cooling to room temperature the mixture had a consistency and appearance of white glue. Poly(ethylene glycol) (1.5 g) reacted with Bisphenol A

diglycidyl ether (MW ~ 15 000 Aldrich) was added and the mixture stirred for an additional 6−8 h. Thin-film electrodes were prepared by depositing a few milliliters of this mixture onto FTO masked with transparent tape, and spreading the material with a glass test tube. After air-drying, sintering is performed in air or oxygen at 450 °C for 30 min. The result is a mesoporous anatase film that is approximately 5−10 μm thick. The materials were then cooled to room temperature and used for sensitizer attachment.

Anchoring the sensitizer to colloidal TiO_2 films simply involves soaking the films in millimolar sensitizer solutions.[21] A common sensitizer series is Ru(II) polypyridyl complexes containing the ligand 4,4′-$(COOH)_2$-2,2′-bipyridine, abbreviated dcb, that can bind to TiO_2 through dehydrative coupling with surface hydroxyl groups to form ester linkages (eq V).[7,23−25] These

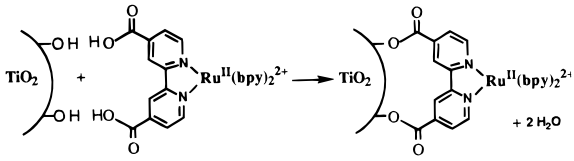

(V)

sensitizers are stable in organic solvent and acidic water, but the sensitizers are rapidly freed in basic aqueous solution. Recently, linkages based on acac and phosphonate groups have been reported.[21,26] The phosphonate linkage is particularly attractive since it is stable in alkaline solution.[26]

While the most widely studied material has been TiO_2, the sol−gel process has been successfully employed in the preparations of other colloidal materials, several of which are ripe for charge separation studies.[27] Thin films of colloidal ZnO were synthesized via careful hydrolysis of zinc acetate producing a porous film consisting of particles 20−50 Å in diameter.[27d] SnO_2 colloidal films, prepared by deposition of commercially available sol (Johnson Matthey) on indium-doped tin oxide coated glass electrodes have been reported.[27e,31]

C. Applications. To date, almost all applications of molecular excited states in sol−gel processed semiconductors have been for solar energy conversion. Wide-bandgap semiconductors, $E_g > 3$ eV, do not appreciably absorb visible light, and the incorporation of molecular chromophores allows efficient solar harvesting. Both organic and inorganic sensitizers have been employed, as discussed below. The most robust and efficient sensitizers are based on the metal-to-ligand charge-transfer (MLCT) excited states of Ru(II) polypyridyl compounds, which have been well reviewed.[28]

Like natural photosynthesis, sensitized sol−gel processed materials convert light into useful energy by efficiently separating charge.[5] Shown in Scheme 1 are the electron-transfer processes that can be initiated when a photon of visible light excites a Ru(II) polypyridyl compound anchored to a TiO_2 particle. Light excitation (1) forms the MLCT excited states that are known to rapidly inject electrons into TiO_2 (2) with a quantum yield near unity under appropriate conditions.[6] This produces an interfacial charge-separated pair with the electron in TiO_2 and the hole localized on the ruthenium metal center. There exist at least two possible fates for this charge-separated pair: recombination to form ground-state products (3) or an external

Scheme 1

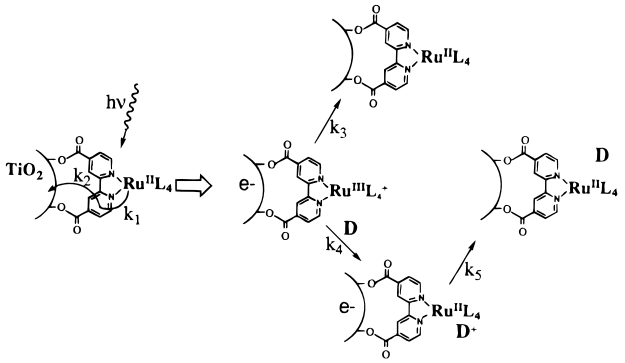

Scheme 2

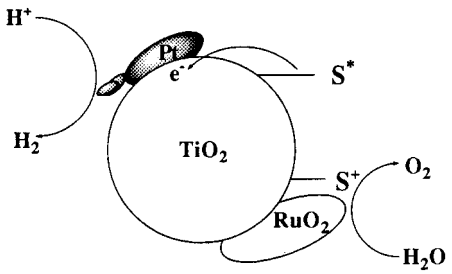

electron donor, D, can reduce the oxidized form of the sensitizer (4). This latter process generally enhances the lifetime of the electron in the solid and moves the hole from the surface-bound sensitizer to a mobile donor that can do work external to the semiconductor surface. The key goals, from an artificial photosynthetic point of view, are to efficiently separate charge (2) and prevent energy wasting back reactions (3) and (5). The k_1-k_5 notation shown in Scheme 1 will be used through out this review.

Studies in the early 1980s attempted to use the interfacial charge-separated state to split water into hydrogen and oxygen in the presence of suitable catalysts (Scheme 2).[29] While the photocatalytic yields were low and reproducibility was a significant obstacle, these studies did elucidate many of the underlying dynamics that promote and inhibit charge separation at sensitized sol−gel interfaces. It is important to emphasize that sustained production of hydrogen and oxygen in these sensitized systems has not been achieved. Efficient water splitting with visible light has long been the holy grail of artificial photosynthetic assemblies and may one day be accomplished.[5] These studies were not restricted to sensitized colloids in aqueous solution. The sol−gel process is sufficiently general that semiconductor particles can be deposited within porous solids.[1] In this manner, chemically integrated assemblies capable of efficiently separating charge may be realized.

As described above, there has been a growing effort to extend colloidal studies to the direct conversion of light into electricity.[6,11,23] To take advantage of nanometer-sized sol−gel processed semiconductor clusters, one must provide an electron pathway for conduction between the particles. This has been achieved by briefly sintering colloidal solutions deposited on conductive substrates. The resultant material is generally a porous nanostructured film which retains many of the characteristics of colloidal solutions but is in a more manageable form. Furthermore, the Fermi level within each semiconductor particle can be controlled potentio-

Scheme 3

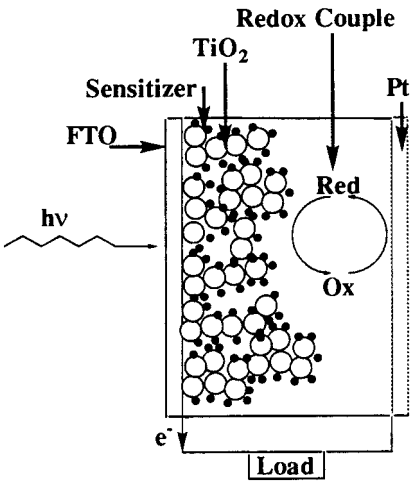

statically.[30−32] Thus both the spectroscopic and electrochemical properties of the material can be probed.

Anchoring molecular sensitizers to the surface of the porous nanostructured film allows visible light harvesting. In fact the long (∼10 μm) path length afforded by the porous nanocrystalline film allows near complete light absorption at wavelengths of light where the sensitizer absorbs strongly. Shown in Scheme 3 is a regenerative solar cell based on these materials. The colloidal materials are deposited on an optically transparent fluorine-doped tin oxide (FTO) support and illumination is through the FTO. When employed in a regenerative solar cell with an appropriate redox couple, these materials convert light into electricity with remarkable efficiency.[6] At individual wavelengths of light, *incident* photons are converted to electrons in the external circuit with near unit efficiency.[23] The electron-transfer processes that allow and inhibit the conversion of photons into electrons are described in Scheme 1. For the most efficient solar cells, iodide is the electron donor, D, which is regenerated at the Pt counter electrode. The solar cell is therefore termed regenerative since no net chemistry occurs. The high efficiency and stability of these cells suggest an economically competitive approach to solar energy conversion.

II. Literature Results

A. Colloidal Solutions. Early spectroscopic studies of semiconductor colloids utilized direct ultraviolet excitation of the solid.[33] Recombination, trapping and interfacial electron-transfer processes were quantified spectroscopically. The results of these studies have been reviewed and will not be discussed further here.[33] In the 1980s, Fox,[34] Kamat,[35] Grätzel,[36] and others began sensitizing TiO_2 colloids to visible light with molecular sensitizers. A key early paper by Grätzel and Moser described the dynamics of charge separation and recombination at a sensitized semiconductor interface for the first time.[13] The sensitizer was eosin Y which has a broad pH-dependent absorption at ∼520 nm. The semiconductor was comprised of ∼50 Å spherical TiO_2 particles prepared from hydrolysis of $TiCl_4$ as described above. At high pH the colloid was stabilized with poly(vinyl alcohol).

At pH < 7.5 a red-shift in the absorption spectrum was attributed to adsorption of the eosin dianion to the colloidal TiO_2 surface. A concomitant red-shift and a dramatic quenching of the luminescence intensity was also observed. The quantum yield for luminescence decreased from 0.22 to ∼0.04 when the pH was decreased from 8 to 2. Time-resolved absorption spectroscopy revealed that electron-transfer quenching occurred from the excited singlet state. Time-resolved resonance Raman studies demonstrate the presence of the oxidized eosin and reveal surface-sensitizer interactions.[37] The triplet state of eosin decays with the same kinetics in free solution and when associated with TiO_2, indicating that interfacial charge separation does not occur from the triplet state.[13] At pH 3 the quantum yield for charge separation was estimated to be 0.4 with rate constant $8.5 \times 10^8\ s^{-1}$. It was found that recovery of the oxidized eosin sensitizer, EO^+, followed complex kinetics. Kinetic analysis with some assumptions yields a charge recombination rate of $2 \times 10^5\ s^{-1}$ and a mean lifetime of interfacial charge-separated states was ∼5 μs. More recent picosecond studies have placed the charge separation rate at $k_2 = 9.5 \times 10^8\ s^{-1}$ and revealed a surprisingly small sensitivity of the charge recombination rate to temperature.[36]

Some important conclusions from this early study proved to be very general and are worth emphasizing.[13] First, for the singlet state of the sensitizer to inject, the sensitizer had to be associated with the TiO_2 particles. This is reasonable considering that organic singlet states are too short-lived for efficient dynamic electron-transfer quenching in dilute solution. Second, the kinetics for charge recombination were approximately 10^3 slower than that for charge separation. As a consequence, the interfacial charge-separated state lives for several microseconds and could potentially undergo secondary redox reactions. These conclusions were largely supported by subsequent work with other organic sensitizers and sol−gel processed colloids.[34−37]

Kamat extended these studies to nonaqueous acetonitrile solution with the sensitizer anthracene 9-carboxylic acid, 9-AC.[35a,b] The TiO_2 particles, prepared from Ti(*i*-OPr)$_4$, were roughly spherical with a mean radius of ∼150 Å. The florescence from 9-AC* was quenched by colloidal TiO_2, and analysis of the quenching data revealed an apparent association constant of $6 \times 10^3\ M^{-1}$.[35] Charge injection again occurred only from the singlet excited state and time-resolved emission revealed $k_2 = 4.8 \times 10^8\ s^{-1}$. Most of the charge-separated states recombined rapidly under these conditions, $k_3 = 4.4 \times 10^7\ s^{-1}$. The small fraction of the charge-separated states that recombined more slowly were able to reduce an organic substrate. Although the quantum yield for reduction was low, this work demonstrated that the interfacial charge-separated states could mediate an organic reduction in acetonitrile solution.

More recent work by Kamat and Patrick have shown that dynamic quenching by wide-bandgap semiconductors can occur.[35] Thionine was used to sensitize 20−40 Å ZnO colloids. Thionine had previously been used to sensitize TiO_2 where a sensitizer−semiconductor interaction resulted in fast charge separation from the singlet state. Here, both the ZnO colloids and the thionine sensitizer were positively charged, precluding such interactions. Therefore, the luminescence and absorption properties of thionine were not significantly altered

by exposure to ZnO. In contrast, the lifetime of the thionine triplet excited state decreases from 88 to 15 μs as the concentration of ZnO colloid was increased, suggestive of interfacial electron transfer. The appearance of the oxidized sensitizer demonstrated an electron-transfer quenching mechanism that proceeds with a quantum yield of 0.1.

Grätzel and co-workers first estimated the rates of interfacial charge separation and recombination with an inorganic sensitizer.[19] The sensitizer was $Ru(dcb)_3(Cl)_2$, using colloidal TiO_2 prepared from $TiCl_4$ as discussed above. At pH 2 the photoluminescence (PL) intensity from the sensitizer was dramatically quenched by the addition of colloidal TiO_2. The lifetime of the excited sensitizer decreased from 600 to 19 ns with some longer components. Laser actinometry indicated that the quantum yield for injection was 0.6 ± 0.1 and the charge separation rate was $k_2 = 3.2 \times 10^7$ s^{-1}. Time-resolved absorption spectroscopy revealed a long-lived transient assigned to the interfacial charge-separated state. Charge recombination occurred with complex kinetics and an average rate constant of $k_3 = 4 \times 10^5$ s^{-1}. Therefore, like previous studies with organic sensitizers, the charge separation process was ~1000 times faster than charge recombination. Interestingly, the PL properties of $Ru(bpy)_3^{2+}$ were not affected by addition of TiO_2 at this pH.

We recently extended these studies with hopes of utilizing the interfacial charge-separated state to oxidize organic promethazine (PMZ) donors.[38] The sensitizer was $Ru(dcb)(bpy)_2^{2+}$ associated with ~5 nm TiO_2 particles prepared from $TiCl_4$ after dialysis to pH 2 (Figure 1). The PL intensity from $Ru(dcb)(bpy)_2^{2+*}$ was quenched by TiO_2 particles. Under these same conditions, the $Ru(dcb)(bpy)_2^{2+*}$ lifetime was constant, indicative of a static quenching mechanism (Figure 2). The data are well described by the Stern−Volmer model from which an adduct formation constant of $K_{ad} = 20 \pm 2$ M^{-1} was calculated. A slight broadening of the visible charge-transfer band of $Ru(dcb)(bpy)_2^{2+}$ is observed upon addition of TiO_2.

Time-resolved absorption spectroscopy allowed the rate constants shown in Scheme 1 to be quantified, Scheme 4.[38] Charge separation occurred within the laser pulse allowing only a lower limit to be assigned. At high concentrations of TiO_2, the quantum yield for charge separation was 0.8. In the absence of PMZ, charge recombination occurred on a tens of microsecond time scale with a mean rate constant $\langle k_3 \rangle$ of ~10^6 s^{-1}. PMZ efficiently intercepts the charge-separated state and reduces the oxidized sensitizer. Significantly, this process shifts the "hole" from the surface-bound sensitizer to a mobile oxidizing equivalent, PMZ^+, that can perform work external to the semiconductor surface. Further, this process increases the lifetime of the charge-separated state to the millisecond time scale. Kinetics for charge recombination of the electron in TiO_2 with PMZ^+ follow a second-order equal concentration kinetic model, k_5.

Recent work by Ford and Rogers have utilized commercially available SnO_2 colloids.[39] It had previously been shown that tin oxide colloid quenches the emission of $Ru(bpy)_3^{2+}$ in alkaline solution.[40] These studies confirm an electron-transfer mechanism for a chemically related sensitizer, $Ru(bpy)_2L^{2+}$, where L = 5-hexadeca-

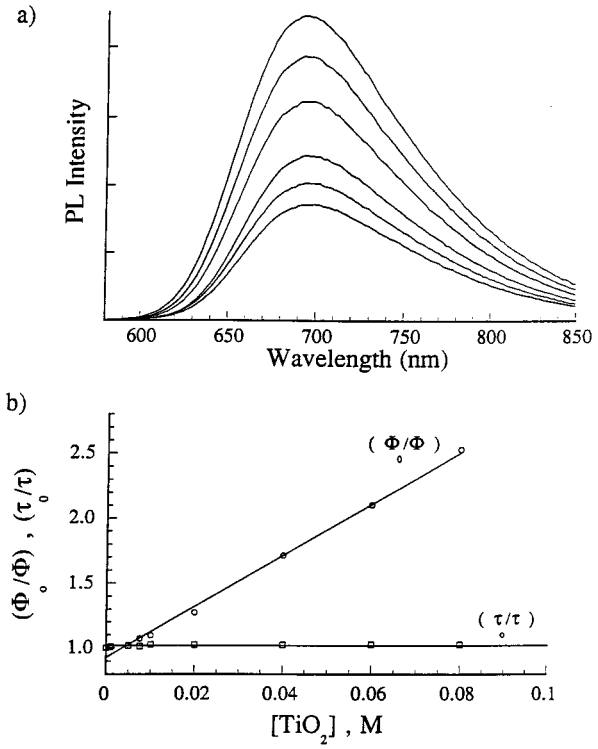

Figure 2. (a) Steady-state quenching of the $Ru(dcb)(bpy)_2^{2+*}$ PL intensity by TiO_2 colloid at pH 2. The excitation wavelength was 460 ± 2 nm. (b) Stern−Volmer analysis of the PL quantum yield (circles) and lifetimes (squares) indicates a static mechanism.

Scheme 4

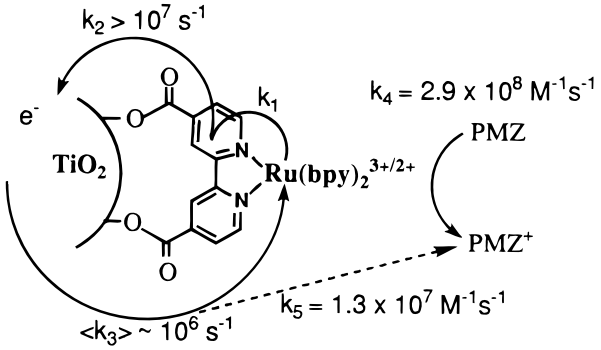

mido-1,10-phenanthroline. Electrostatically and covalently bound assemblies were explored using time-resolved spectroscopy. The rate of charge separation was much faster, $> 2 \times 10^7$ s^{-1}, than charge recombination. The charge recombination kinetics were fit to a distribution model with average rate constants on the 10^5−10^6 s^{-1} time scale. These studies were later extended to surfactant bilayers with the cationic didodecyldimethylammonium ion, $DDMA^+$, and a zwitterion, 1,2-dioctanoyl-*sn*-glycero-1-phosphocholine with 1,1′-di-*n*-hexadecyl-4,4′-bipyridinium ion, CV^{2+}. Light excitation of the Ru(II) sensitizer led to rapid electron transfer to SnO_2 followed by electron transfer to CV^{2+}. Charge recombination from $CV^{\bullet+}$ to $Ru^{III}(bpy)_2L^{3+}$ was an order of magnitude slower than that observed from $SnO_2(e^-)$. Efficient charge separation coupled with slow charge recombination and the commercial availability of the SnO_2 colloids make these assemblies attractive for applications in photocatalysis.[39]

An advantage of the sol−gel process is that it allows wide-bandgap semiconductor materials to be deposited

Scheme 5

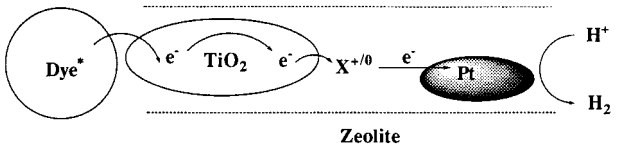

in different materials. The incorporation of colloidal TiO_2 into zeolite materials and subsequent dye sensitization has been achieved.[41] Platinated linear channel zeolites were loaded with TiO_2 by the hydrolysis of titanium tetraalkoxide or $TiCl_4$. In addition, Nb_2O_5 particles were deposited by a sol−gel process from $NbCl_5$ or $Nb(OMe)_5$(pyridine) precursors. Note that the semiconductors were deposited on both external and internal surfaces of the zeolite. The zeolites were next loaded with $Ru(dcb)_3Cl_2$ and then with methylviologen (MV^{2+}) as an electron shuttle. The resulting composite is a dye sensitized semiconductor trapped inside a zeolite with platinum patches and an electron shuttle to transport electrons from the semiconductor to the platinum, where it is hoped water reduction to hydrogen gas might occur. A pictoral representation of the idealized assembly is shown in Scheme 5 .

When the size-excluded photosensitizer was adsorbed onto the surface of TiO_2 and Nb_2O_5, the photoluminescence was quenched. Charge separation in the $Ru(dcb)_3/TiO_2$/zeolite system occurred within the laser pulse. Charge recombination was measured by diffuse reflectance transient absorption spectroscopy for the TiO_2 assembly. For both zeolite materials, charge recombination was about 100 times slower, $k_3 \sim 10^3\ s^{-1}$, than that measured by Grätzel and co-workers in aqueous colloidal solution.[19] Addition of iodide shuttles the hole from the oxidized sensitizer to I^- that forms $I_2^{\bullet -}$ and prolongs the lifetime of the charge-separated pair to the millisecond time scale. Cation exchange of MV^{2+} or dicyanomethylviologen (DCV^{2+}) was performed to collect the electrons in TiO_2. DCV^{2+} was reduced by $TiO_2(e^-)$ to form the charge-separated state, $Ru^{III}(dcb)_3/TiO_2$/zeolite ($DCV^{\bullet +}$), that has a lifetime of ~120 μs. Interestingly, the electrons in TiO_2 were unable to reduce MV^{2+} under these conditions. A hydrogen evolution quantum yield was measured to be 1% with sacrificial electron donors. The sensitized Nb_2O_5 particles did display a small yield of hydrogen with reversible electron donors.[41]

B. Colloidal Thin Films. The art and science of sensitizing colloidal sol−gel processed metal oxide films stems from early work done with single-crystal electrodes in the 1970s and early 1980s.[7−10] The poor light-harvesting efficiency of a sensitizer monolayer on a flat single-crystal surface produced photocurrent in a low and impractical yield. Sensitization of high surface area materials allows high light-harvesting efficiency that increased the solar conversion efficiency significantly. This work culminated with the report by Grätzel and O'Regan of a 7.5% efficient solar cell under simulated sunlight conditions.[6] The efficiency, stability, and low-cost processing suggested an economically competitive approach to solar energy conversion. This breakthrough was realized by significant advances in supramolecular sensitizer design, sol−gel processing, and electrolyte modification.

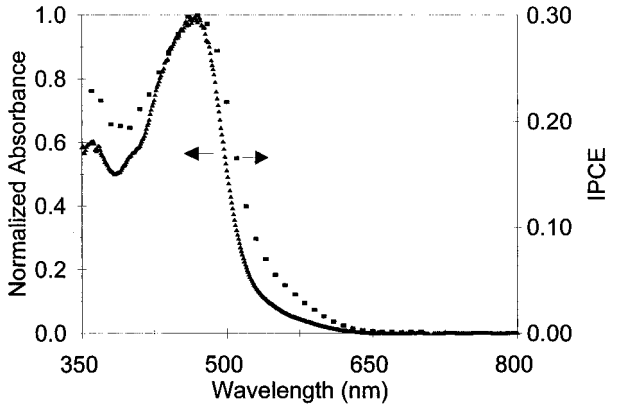

Figure 3. Photocurrent action (squares) and absorbance (triangles) spectra of $Ru(dcb)(bpy)_2^{2+}$ anchored to a nanocrystalline TiO_2 film. The photocurrent action spectra was recorded in 0.5 M LiI, 0.05 M I_2 in acetonitrile where the IPCE is the incident-photon-to-current efficiency. The absorbance spectra was recorded in 0.1 M $LiClO_4$ acetonitrile electrolyte.

The preparation of sensitized nanocrystalline TiO_2, ZnO, and SnO_2 films for sensitization studies have been discussed in the Introduction and Background section. The interfacial electron-transfer processes that allow (and inhibit) the light-to-electrical energy conversion are shown in Scheme 1. For simplicity it is worthwhile to consider these processes sequentially. Since the most efficient and widely studied sensitizers for this application have been Ru(II) polypyridyl compounds, we will focus the discussion on these sensitizers.

1. Charge Separation (k_2). The high light-to-electrical energy conversion efficiency measured in regenerative solar cells demonstrates that electron transfer from the excited sensitizer to colloidal semiconductors can occur with a quantum yield of unity.[6] Photocurrent action spectra, plots of photocurrent efficiency versus excitation wavelength, closely resemble the absorption spectra of the sensitizer, indicating that MLCT excitation occurs before electron injection as shown in Scheme 1.[6] A representative absorption and photocurrent action spectra are shown in Figure 3. Most direct methods for estimating the rate of charge separation were limited by instrumental response times and revealed only a lower limit, $k_2 > 10^7\ s^{-1}$. Early work used time-resolved PL to indirectly measure charge-separation rates.

The PL properties of Ru(II) polypyridyl sensitizers on nanocrystalline supports were recently reviewed.[42] Interestingly, despite gross differences in particle sizes, sensitizers, and surface−sensitizer interactions, the time-resolved PL data from the charge-transfer sensitizers are remarkably similar. The different rates available in the literature therefore largely reflect differences in analysis. The electron-transfer rate was calculated as the difference between the sensitizer excited-state lifetimes on the semiconductor, τ_{sc}, and a substrate where electron transfer does not occur, τ_{ins} (eq VI). In

$$k_2 = 1/\tau_{sc} - 1/\tau_{ins} \qquad \text{(VI)}$$

practice, sensitizer lifetimes on insulators are so much longer lived than those on semiconductor materials that $k_2 \sim 1/\tau_{sc}$. The main assumptions in the use of eq VI is that electron transfer is the only quenching mechanism on the semiconductor not present on the insulator and that the sum of the radiative and nonradiative decay

components ($k_r + k_{nr}$) of the sensitizer is independent of substrate. A significant difficulty in quantifying the PL decays from excited sensitizers anchored to sol−gel processed particles is the appearance of complex kinetics. The decays do not follow first-order kinetics, and discrete lifetimes therefore do not exist.[42] It has largely been assumed that the complex kinetics are a result of underlying heterogeneity and the decay kinetics are modeled as a sum of discrete rates. In some cases, as many as four rates and therefore eight parameters are required to accurately model the data. The difficulty with this approach is that highly correlated parameters with significant experimental uncertainty are obtained. Furthermore, the rates may have little real meaning if the kinetics are actually a result of an underlying distribution.

The recovery of distributions of lifetimes or rates from temporal data is nontrivial. The problem is closely related to the inversion of Laplace transforms which is inherently ill-conditioned.[43] A recent distribution analysis of the PL decays from Ru(dcb)(bpy)$_2^{2+}$, *cis*-Ru(dcb)$_2$(CN)$_2$, and *cis*-Ru(dcb)$_2$(NCS)$_2$ anchored to nanocrystalline TiO_2 in operational solar cells and ZrO_2 under the same conditions was reported.[42] In analyzing time-resolved PL data, the recovered decays were modeled with a variety of analytical distributions that represent the underlying amplitude distribution. It was found that symmetric distributions such as Gaussian, Lorentzian, or uniform distribution with appropriate signal-to-noise, were unable to model the data. However, the Albery and Kohlrausch−Williams−Watts (KWW) models,[44] which are based on log-normal and Levy distributions of decay rates respectively, will. It is the skewness or asymmetry of these distributions that is significant, and it is likely that many other skewed distributions will model these data equally well.[42]

A shortcoming of a distributional approach is the a priori assumption of a continuous distribution of rates. In principle this shortcoming can be overcome through the use of regularization techniques such as maximum entropy analysis.[45] However, the validity of any regularization procedure is an unresolved issue. An advantage of the distributional approach is that only two parameters are required to fit all the normalized data. These parameters are not highly correlated and a well-defined error surface is obtained. Further, if one accepts that the complex PL decays do represent underlying dispersive kinetics, the inverse Laplace transforms are known and the distributions can be recovered. In this manner some insights into the underlying physical processes may be obtained when a larger base of experimental data is available. Further, for estimating charge separation rates, distributions of lifetimes can be utilized with eq VI. The results for the Albery model applied to the sensitizer Ru(dcb)(bpy)$_2^{2+}$ anchored to nanocrystalline TiO_2 are shown in Figure 4. The rates reveal a broad distribution of charge-separation rates with peak amplitude $\sim 10^9-10^{10}$ s^{-1}. To date, these are the only estimates of the electron injection rates in operational high-efficiency solar cells.[42] It is important to emphasize, however, that PL is an indirect method for measuring electron-transfer rates and is subject to the uncertainty of the assumptions described above.

Kamat and Fessenden have examined the PL properties of the sensitizer Ru(dcb)(bpy)$_2^{2+}$ anchored to colloidal ZnO, TiO_2, and SnO_2 films and have estimated the rate of electron injection from these data.[46] PL decays at 650 nm were modeled as a biexponential decay, with an approximate order of magnitude difference between the fast and slow rate. Following selective excitation of the sensitizers, direct evidence for electron injection came from an absorption growth in the microwave region assigned to conduction band electrons. For SnO_2 and ZnO, the microwave kinetics agreed well with the electron injection rates from PL quenching measurements. The electron-transfer rates were calculated from these data, $k_2 = (1-3) \times 10^8$ s^{-1}. It is not clear how charge trapping and detrapping may affect the microwave absorption change measured. The calculated electron-transfer rates showed an interesting correlation with the energy difference between the sensitizer excited-state oxidation potential and the energy of the semiconductor conduction band edge (ΔE in Scheme 6). The rate was found to increase with ΔE. In fact, the raw experimental data reflects this: the larger ΔE, the faster the PL decays to baseline. A similar behavior had previously been observed for sensitized semiconductor powders.[47] Further, if the pseudo-Fermi level in TiO_2 nanocrystalline films is shifted positive with an externally applied potential, the rate of electron injection increases from that observed at more negative potentials.[31] Charge separation, therefore, appears to be sensitive to sensitizer and semiconductor energetics in a manner that is not easily rationalized.

Very recently, a femtosecond time-resolved absorption study of *cis*-Ru(dcb)$_2$(NCS)$_2$ anchored to a nanocrystalline TiO_2 film in 1:1 ethylene carbonate/propylene carbonate solvent was reported.[48] The authors were

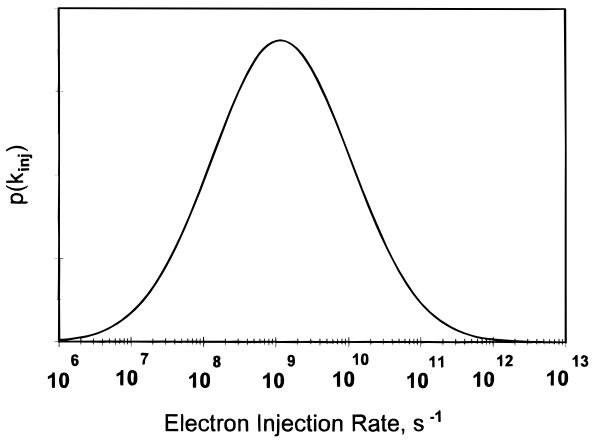

Figure 4. Distribution of electron injection rates for Ru(dcb)(bpy)$_2^{2+}$ anchored to a nanocrystalline TiO_2 film in a regenerative solar cell with 0.5 M NaI/0.05 M I_2 in proylene carbonate. The electron injection rates, k_2 in Scheme 1, were calculated through a distribution analysis of the time-resolved PL decays monitored at 700 nm as described in the text.

Scheme 6

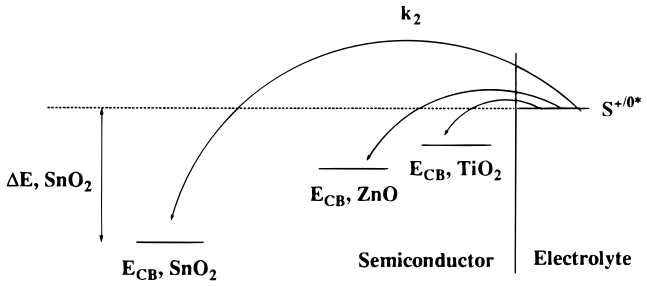

able to spectroscopically observe both halves of the interfacial charge-separated pair, the oxidized sensitizer and the electron in TiO_2. Unfortunately, at long observation wavelengths, $\lambda = 650-900$ nm, these absorption features overlapped with each other and with excited-state absorption, making assignments and analysis difficult. Detailed analysis of the transient absorption data indicate that the electron injection process is at least biphasic with ~50% injecting in less than 150 fs and 50% in 1.2 ps. The results suggest that under appropriate conditions, interfacial charge separation can be very fast, perhaps occurring from the Franck–Condon state.[50] This important conclusion should allow new classes of sensitizers with very short excited-state lifetimes to be utilized for efficient interfacial charge separation.

For all the sensitizers cited above light excitation is localized on the surface-bound dcb ligand. Goodenough first proposed that the ester linkage should enhance electronic coupling between the π^* orbitals of the bipyridine ring and the Ti 3d orbital manifold of the semiconductor.[7] In support of this, a comparison of the solution absorption spectrum with the photoaction spectrum on rutile reportedly reveals a significant red-shift upon surface attachment.[49] A similar energy shift was observed for *cis*-$Ru(dcb)_2(NCS)_2$ anchored to anatase nanocrystalline films,[52] which is consistent with stabilization of the MLCT excited states by the TiO_2 surface. Recent vibrational studies support the presence of surface ester bonds.[24] However, whether this linkage increases charge-separation efficiency or promotes electronic coupling between the sensitizer and the surface remains largely unknown. Further, whether the sensitizer need be covalently bound to the semiconductor surface remains unknown.

Sensitizers where the surface anchor is not directly coupled to the chromophoric ligand have allowed these issues to be addressed. For example, the photoelectrochemical properties of Ru(II) polypyridyl sensitizers that contain a propylene spacer between the bipyridine ligand and the surface anchoring group reveal monochromatic photon-to-current efficiencies of 0.3–0.5.[21] Further, time-resolved absorption measurements were unable to resolve the rate of electron injection, $k_2 > 10^7$ s^{-1}. However, the spacer is flexible, and the orientation of the sensitizer with respect to the surface is unknown. Nevertheless, the results indicate that a direct linkage between the chromophoric ligand and the semiconductor is not a strict requirement for efficient charge separation at these interfaces.

In an effort to achieve improved molecular control of sensitizer orientation, bimetallic coordination compounds based on rhenium and ruthenium were explored where the facial geometry of the Re center holds a Ru sensitizer proximate to the TiO_2 surface, Scheme 7.[51] Recently, the photophysical and photoelectrochemical properties of two Re–(CN)–Ru linkage isomers anchored to nanostructured TiO_2 films were reported. The results demonstrate rapid efficient interfacial electron transfer and a remarkably high light-to-electrical energy conversion even though the sensitizer is remote to the semiconductor-bound ligand. Therefore, a direct chemical bond between the chromophoric ligand of Ru(II) sensitizers and the TiO_2 surface does not appear to be a requirement for efficient charge separation. While it could be argued that these supramolecular sensitizers represent a special case, this scenario appears unlikely. For example, the photoelectrochemical properties of Ru(II) polypyridyl sensitizers that contain a propylene spacer between the bipyridine ligand and the surface anchoring group reveal monochromatic PCEs of 0.3–0.5, as discussed above.[21] Further, in the original report of sensitization of rutile single crystals by Ru(II) polypyridyl sensitizers, Clark and Sutin concluded that the quantum yield for electron injection from $Ru(4,7\text{-}(CH_3)_2\text{-}1,10\text{-phenanthroline})_3^{2+*}$ is close to unity despite a low photocurrent observed.[8d] It therefore appears that efficient electron injection from MLCT excited states to TiO_2 can occur in the absence of *any* semiconductor-to-sensitizer link. An important implication from this conclusion is that sensitizers anchored to TiO_2 through nonchromophoric ligands or without a direct chemical bond may also be efficient for sensitization of wide-bandgap nanocrystalline semiconductors.

Scheme 7

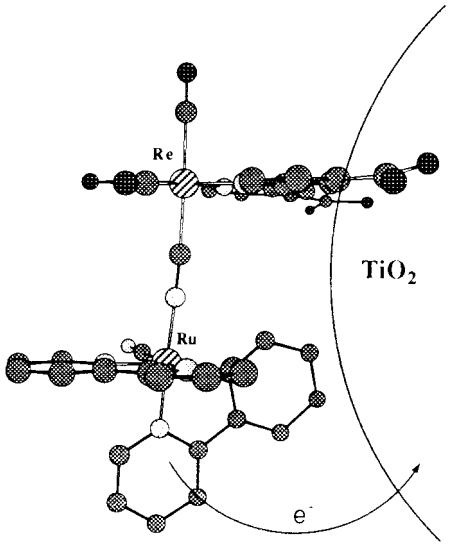

2. Charge Recombination (k_3). Electron transfer from the semiconductor to the oxidized sensitizer wastes the energy stored in the charge-separated state. Initial studies of sensitized TiO_2 colloids revealed that this process occurs on a tens of microsecond time scale. Recombination occurs on this same time scale, $k_3 \sim 10^5-10^6$ s^{-1}, for nanocrystalline TiO_2 and SnO_2 films with Ru(II) sensitizers that have oxidation potentials between ~0.8 and 1.1 V vs SCE.[21,27,51,53] Organic sensitizers recombine on this, or slightly faster, time scales.[54,55]

Therefore, charge separation is 3–5 orders of magnitude faster than charge recombination, $k_2/k_3 > 10^3$. This difference in interfacial electron-transfer kinetics largely underlies the high efficiency of solar cell based on sol–gel processed colloids. The question then naturally arises, why is the back reaction so slow relative to the forward electron-transfer rate? While a clear answer to this question is not known, several possibilities have been suggested in the literature.[23] Since different molecular orbitals are involved in the forward and reverse electron-transfer processes, different rates are expected. Electron injection occurs from the π^* levels of the bipyridine ligand while back electron transfer occurs to the t_{2g} orbitals of the Ru(III) center. The thermodynamic driving force for the two processes are not easily calculated since the nature and energetics of

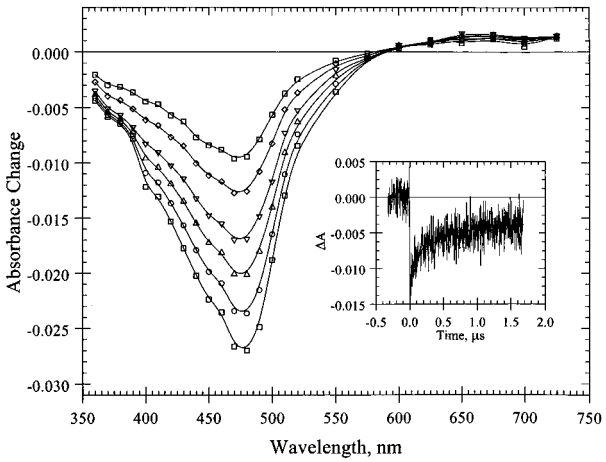

Figure 5. Time-resolved absorption difference spectra recorded after pulsed light excitation (532 nm, ~1 mJ/cm^2, 8 ns fwhm) of a Ru(dcb)(bpy)$_2$/TiO$_2$ film in 0.1 M LiClO$_4$ acetonitrile solution. The absorption spectra corresponds to the oxidized sensitizer and were recorded at 10 ns (squares), 25 ns (circles), 50 ns (triangles), 100 ns (upside down triangles), 400 ns (diamonds), and 1.00 μs (squares). The inset shows the time-resolved absorption monitored at 402 nm that corresponds to k_3 in Scheme 1.

the redox-active state(s) in TiO$_2$ remain unknown. However, there exists some evidence that the back reaction falls in the Marcus inverted region for related sensitizers[36b,56] while the forward reaction may be activationless.[57] The driving force dependence of k_3 will be discussed further below.

In sensitized single-crystal materials, the back reaction is thought to be inhibited by the electric field region at the semiconductor surface.[10] More specifically, the semiconductor depletion region sweeps the injected electron toward the bulk and away from the oxidized sensitizer, thereby inhibiting the back reaction. The extent to which similar processes might occur in the nanostructured materials described here is unknown but is expected to be much less. The application of models developed for bulk semiconductors to colloidal materials is not straightforward, especially when the semiconductor particle is very small.[32] The small size severely restricts the magnitude of the electric field a particle can support and concepts such as depletion or accumulation layers may not be generally applicable.[58] Further, charge recombination measurements made under potentiostatic conditions fail to reveal any electric field dependence for this process,[31] as discussed further below.

An important aspect of the charge-recombination process is its dependence on thermodynamic driving force. Currently there exists no consensus on whether k_3 falls in the Marcus normal or kinetic inverted region, and evidence for both has been advanced in the literature.[36,56,59] Part of the difficulty in addressing this issue lies in modeling the complex kinetics observed spectroscopically after selective excitation of the surface bound sensitizer. The inset in Figure 5 shows a time-resolved absorption bleach that corresponds to reduction of Ru^{III}(dcb)(bpy)$_2$/TiO$_2$ by electrons in TiO$_2$, k_3. Approximately two-thirds of the signal recovers in the first 1.5 μs, and the remaining signal (not shown) recovers on a tens of microseconds time scale. The data cannot be fit to a first- or second-order kinetic model but can be described by a sum or distribution of first-order rate constants. As stated previously, average rate constants $k_3 \sim 10^5$–10^6 s^{-1} have generally been reported for Ru(II) polypyridyl sensitizers.[21,27,51,53]

The sensitizers *cis*-Ru(dcb)$_2$(CN)$_2$ and *cis*-Os(dcb)$_2$(CN)$_2$ anchored to sol–gel processed TiO$_2$ and DeGussa TiO$_2$ provide an interesting comparison since the oxidation potential of the Ru(II) sensitizer is 340 mV more positive than that of the Os(II) sensitizer.[59] Therefore, assuming a common donor state(s) in TiO$_2$, the driving force for charge recombination should be 340 mV larger for the Ru(II) sensitizer.[59] However, average rate constants estimated from diffuse reflectance data for a large number of sensitized materials were, within a factor of 2, the same.[64] In addition, charge recombination for bimetallic Re–(CN)–Ru linkage isomers described above are within experimental error the same, despite a 130 mV difference in driving force, $\langle k_3 \rangle = 3 \pm 1 \times 10^5$ s^{-1}.[51]

Hupp and co-workers have found that the fast component of an absorption transient, assigned to charge recombination, was insensitive to pH over 13 decades of H$^+$ concentration. For single-crystal electrodes the flat-band potential is known to shift 59 mV/pH unit. Assuming the sensitizer oxidation potential is pH independent and that electron transfer occurs from a TiO$_2$ donor state that also displays this pH dependence, the driving force for charge recombination should have been varied by over 470 mV. Yet there was no observed change in the kinetics of the fast component.[60] More recent data suggest that the sensitizer oxidation potential may also be pH dependent when anchored to the semiconductor surface.[61] More studies are needed before this interesting interfacial behavior can be fully understood.

Another strategy for slowing charge recombination is to apply an electric field to the nanocrystalline film. In this manner the Fermi level within each semiconductor particle can be controlled and possible changes in recombination kinetics can be monitored.[30,31] Kamat and co-workers found that the charge-recombination kinetics observed after excitation of Ru(dcb)(bpy)$_2$/SnO$_2$ at different applied potentials were within experimental error the same.[31] A potential-independent charge-recombination process was observed on a tens of microseconds time scale. An interesting observation from these studies, and others with sensitized TiO$_2$,[30,42] is that the charge-separation yield decreased as the Fermi level in the colloidal film was shifted toward the vacuum level. The decreased injection yield manifests itself in an increase in PL intensity and sensitizer excited-state lifetime. This behavior is unexpected. The decreased photocurrent observed near the flat-band condition in sensitized single-crystal materials is not thought to be due to a decreased quantum yield for electron injection. Instead, excited-state electron transfer occurs, but the lack of a substantial surface electric field results in rapid recombination and inefficient photocurrent production.[10] It therefore appears that the increased PL quantum yield is a special feature of sensitized nanocrystalline metal oxide semiconductors. It remains unclear why the quantum yield for charge separation decreases with negative applied potentials; however, a trap filling and/or decreased sensitizer–semiconductor electronic coupling have been suggested.[42]

Scheme 8

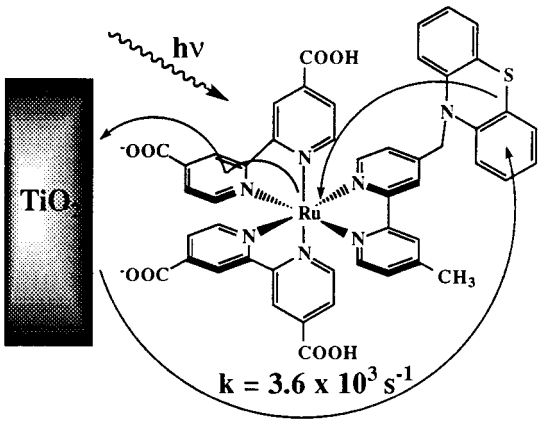

One strategy to increase charge-separation lifetimes is to covalently bond a secondary donor to the Ru(II) sensitizer. This strategy was explored with the sensitizer, [Ru(dcb)$_2$(bpy-PTZ)], shown in Scheme 8.[62] Less than 20 ns after excitation of the surface-anchored [Ru(dcb)$_2$(bpy-PTZ)] sensitizer, an electron is injected into TiO_2 and the PTZ group reduces the metal center. It is unclear which happens first. The net effect is to shift the "hole" from ruthenium to the pendent PTZ group by rapid intramolecular electron transfer. These excited-state electron-transfer reactions produce interfacial charge-separated pairs that are remarkably long-lived, $k = 3.6 \times 10^3$ s^{-1}. Visible excitation of a model compound that does not contain PTZ, Ru(dmb)(dcb)$_2$/TiO_2, under the same conditions results in the formation of an interfacial charge-separated state that recombines with complex kinetics and an average rate, $\langle k_3 \rangle = 3.9 \times 10^6$ s^{-1}. Therefore, the recombination rate is slowed by $\sim 10^3$ by translating the "hole" from the metal center to the pendent PTZ group. Further studies are required to ascertain whether the long lifetime of the charge-separated states results from orientation of the PTZ$^+$ group, a change in driving force, and/or spin effects.

When employed as a photoanode in a regenerative solar cell with iodide as an electron donor, [Ru(dcb)$_2$(bpy-PTZ)]/TiO_2 efficiently converts photons into electrons. For a large number of samples the IPCE is 45 ± 10%, which is within experimental error the same as that observed for Ru(dcb)$_2$(dmb)/TiO_2 photoanodes measured under the same conditions. A key difference in the photoelectrochemical properties, however, is an $\sim$100 mV larger open-circuit photovoltage, V_{oc}, for [Ru(dcb)$_2$(bpy-PTZ)]/TiO_2 when compared to Ru(dcb)$_2$(dmb)/TiO_2, which serves as a model. V_{oc} defines the maximum Gibbs free energy that can be obtained from a photoelectrochemical cell under constant light irradiance conditions.[65] The maximum open-circuit photovoltage attainable is the energetic difference between the Fermi level of the solid under illumination and the Nernst potential of the redox couple in the electrolyte. However, this maximum has not been realized, and there is growing evidence that V_{oc} is kinetically limited by electron tunneling through the solid to the oxidized form of the dye and/or the electron donor.[66]

Lewis and co-workers have examined the factors that control open-circuit voltages in regenerative photoelectrochemical cells based on crystalline Si materials in great detail.[67] They find that V_{oc} is not a thermodynamic quantity but rather a kinetic variable of a photostationary state. For an n-type semiconductor the open-circuit voltage is the potential at which the majority carrier current density due to electron injection from the conduction band (I_{inj}) exactly offsets the photogenerated interfacial hole current density from the valence band. Equation VII and modified forms, often

$$V_{oc} = \left(\frac{kT}{e}\right) \ln\left(\frac{I_{inj}}{n \sum_i k_i [A]_i}\right) \qquad \text{(VII)}$$

referred to as diode equations are applicable where n is the concentration of electrons in the semiconductor, and k_i is the electron-transfer rate to acceptor A_i.[67]

If one assumes that I_{inj} is the same for [Ru(dcb)$_2$(bpy-PTZ)]/TiO_2 and Ru(dcb)$_2$(dmb)/TiO_2, than the measured interfacial kinetics and eq VII predict a 200 mV larger V_{oc} for [Ru(dcb)$_2$(bpy-PTZ)]/TiO_2. In fact the measured open-circuit voltage in the absence of iodide is 180 ± 30 mV over 4 decades of irradiance, in excellent agreement with the calculated value.[38] It therefore appears that the molecular charge recombination rates can be directly related to the open-circuit photovoltage of an operational solar cell.[38,62]

3. Donor Redox Chemistry, k_4 and k_5. Surprisingly few studies have utilized the interfacial charge-separated state to oxidize a donor, k_4, and monitor the subsequent recombination, k_5.[38,63] Phenothiazine donors with Ru(dcb)(bpy)$_2$/TiO_2 nanocrystalline films have been employed in this regard.[38] Visible light excitation of Ru(dcb)(bpy)$_2$/TiO_2 rapidly forms the interfacial charge-separated state as discussed above. Phenothiazine donors efficiently intercept the charge-separated state and reduce the oxidized sensitizer in propylene carbonate electrolyte. The bimolecular electron-transfer rate was measured to be $k_4 = 3.2 \times 10^8$ M^{-1} s^{-1}. Significantly, at high phenothiazine concentrations all the oxidized sensitizers in the nanocrystalline film could be accessed by the donors within experimental error. Recombination of the electron in TiO_2 with the oxidized phenothiazine followed a second-order equal concentration kinetic model under the same conditions. Uncertainties in the appropriate optical path length lead to a systematic error in calculated rate constants. However, k_5 was approximately 10^7−10^8 M^{-1} s^{-1}, consistent with colloidal solution studies where the path length was better defined. Unfortunately, the recombination process is very efficient and oxidized phenothiazines are unable to escape the sensitized TiO_2 network. Therefore, the use of phenothiazine donors in regenerative solar cells results in negligible photocurrent production.[38]

Preliminary estimates of k_4 with iodide as the donor were made by diffuse reflectance and absorption spectroscopy of the fractal TiO_2, Degussa, and transparent anatase films sensitized with *cis*-Ru(dcb)$_2$(CN)$_2$ and *cis*-Os(dcb)$_2$(CN)$_2$.[64] The recovery of the charge-transfer bleach, after selective excitation of the sensitizer, was measured in the presence and absence of 0.5 M I$^-$. The addition of 0.5 M I$^-$ resulted in the prompt recovery for the Ru(II) sensitizer but had a much smaller effect on the kinetics for the Os(II) sensitizer. The prompt recovery of the Ru(II) state results from rapid iodide oxidation, and the data were used to estimate that rate, $k_4 = 2 \times 10^7$ s^{-1} at 0.5 M NaI in propylene carbonate. The slow recovery of the Os(II) sensitizer in the

presence of 0.5 M I^- explains why the *cis*-$Os(dcb)_2(CN)_2$ sensitizer produced a lower photocurrent in regenerative solar cells with iodide;[59] a sluggish iodide oxidation rate allows efficient charge recombination k_3 to occur.

An issue that remains unanswered is what prevents recombination of electrons in TiO_2 with oxidized iodide products? Perhaps the most remarkable aspect of the efficient solar cells based on these materials is that injected electrons are able to diffuse through the TiO_2 network without recombination. Recently it has been found that V_{oc} increases when pyridine and other adsorbates are exposed to the TiO_2 surface.[66] This suggests that these adsorbates slow recombination of electrons trapped in TiO_2 with iodine acceptors (eq VII).[66] Therefore, k_5 may be very sensitive to surface composition. Direct spectroscopic proof of a decreased recombination rate is still lacking. In addition, the absolute rate constant and the chemical species that participate in this redox chemistry are unknown. Clearly, for phenothiazine donors (and presumably other outer sphere electron donors)[68] recombination is efficient and little measurable photocurrent results.[38]

III. Conclusions

The literature results reviewed here reveal efficient charge separation at sensitized sol−gel processed semiconductor interfaces. Remarkably, the quantum yield for charge separation can be close to unity for a wide variety of sensitizers and colloidal semiconductor particles. Further, the charge separation rate is often 10^2−10^6 times faster than the charge recombination process. This fortuitous difference in rates, coupled with high solar light harvesting, largely underlies the efficiency of regenerative solar cells based on this technology. The interfacial charge-separated states can also be utilized to generate hydrogen fuel in photocatalytic assemblies.

The efficient solar cells that have recently been realized with sensitized sol−gel processed nanocrystalline semiconductor films has encouraged experimental activity in this area. Some recent observations include the realization of ultrafast charge separation which suggests that new classes of sensitizers with very short excited-state lifetimes may efficiently separate charge.[48] Organic sensitizers can be quite efficient, but suffer from poor long-term stability.[54,69] Inorganic, sensitizers based on Ru(II) polypyridyl coordination compounds anchored to nanocrystalline TiO_2 materials display the most favorable combined efficiency and stability.[6] Lately, results suggest that a covalent linkage between the sensitizer and the semiconductor is not a requirement for efficient charge separation.[21,51] In fact, an undetermined sensitizer−semiconductor orientation may exist where charge separation still occurs with a quantum yield near unity, but the back reaction is further inhibited thereby yielding higher open-circuit photovoltages in regenerative solar cells. Charge recombination rates are typically 10^5−10^6 s^{-1} (depending largely upon the model used to describe them) and appear to be insensitive to pH or the Fermi level in the semiconductor particles under potentiostatic conditions.[31,60] The charge recombination rate can be slowed substantially by translating the "hole" from the metal center to a pendent organic donor.[38,62]

This summary reveals that interfacial charge separation and recombination at sensitized sol−gel processed interfaces are becoming reasonably well understood. However, important issues remain unresolved. Still lacking is a reasonable model to account for the complex charge recombination kinetics. Basic information, such as the order of this process, remains generally unknown. Further, what prevents rapid and efficient recombination of injected electrons with oxidized iodide products? What is particularly needed is detailed information concerning the chemical nature and energetics of the redox active states in the semiconductor material. Traditionally, band theory has described the electronic and optical properties of semiconductor materials phenomenally well.[70] However, it is not clear that band theory provides useful insights for these materials and interfacial processes. In fact, there exists very little experimental evidence for delocalized conduction band electrons in any of the sol−gel processed materials reviewed here. It is becoming increasingly apparent that localized surface state(s) may participate in interfacial electron transfer and in the conduction process.[32,71] In TiO_2, the presence of localized redox-active Ti^{III} states is well documented, although the coordination sphere and oxidation potentials remain speculative.[72] In principle, sol−gel science can give unique insights into these molecular semiconductor issues. The high surface area afforded by these materials should make absolute identification of surface states more facile than in single-crystal materials. Once resolved, experimental data on interfacial charge separation, carrier transport, and the potential distribution within the nanocrystalline films can be more fully rationalized.

An important area for future studies is with alternative sol−gel processed semiconductors. To date, the only materials studies in detail are binary oxides SnO_2, TiO_2, and ZnO. Ternary materials such as $SrTiO_3$ or $BaTiO_3$ and other wide-bandgap semiconductors are ripe for study. In addition, the sol−gel process allows the preparation of semiconductor heterostructures, where one or more semiconductor material is coated onto another.[73] Such materials in principle could allow charge to be directed away from or toward the oxidized sensitizer. Preliminary photophysical results and photocatalysis with these novel structures have just begun to appear in the literature.[74]

As stated at the outset, the vast majority of studies have been initiated with solar energy conversion in mind. However, other applications do exist. The dramatic color changes that accompany interfacial electron transfer could be utilized in optical switches and storage devices, for example.[75] Photochromic windows based on this property have in fact recently appeared.[76] Also, the materials can electroluminesce, opening potential applications in luminescent displays.[77]

In conclusion, sol−gel processed semiconductors materials allow one to explore the fate of molecular excited states both spectroscopically and electrochemically. Fundamental studies may ultimately lead to molecular control of excited-state processes at these fascinating interfaces. The potential molecular applications that exist and fundamental intellectual issues that remain ensure a bright future for further research at sensitized sol−gel processed semiconductor materials.

Acknowledgment. We would like to thank the National Science Foundation (CHE-9322559, CHE-9402935), and the Division of Chemical Sciences, Office of Basic Energy Sciences, Office of Energy Research, U.S. Department of Energy for research support. T.A.H. acknowledges support from a Sonneborn fellowship.

References

(1) (a) Roy, R. *Science* **1987**, *238*, 1664. (b) Hench, L. L.; West, J. K. *Chem. Rev. (Washington, D.C.)* **1990**, *90*, 33. (c) Brinker, C. J.; Scherer, G. W. *Sol−Gel Science*; Academic Press: New York, 1991.
(2) Gerfin, T.; Grätzel, M.; Walder, L. *Prog. Inorg. Chem.* **1997,** *44*, 3345.
(3) (a) Gerischer, H. *J. Phys. Chem.* **1991**, *95*, 1356. (b) Fox, M. A.; Chanon, M. *Photoinduced Electron Transfer* Elsevier: Amsterdam, 1988. (c) Grätzel, M. *Heterogeneous Photochemical Electron Transfer;* CRC: Boca Raton, FL, 1989.
(4) (a) Slama-Schwok, A.; Avnir, D.; Ottolenghi, M. *Photochem. Photobiol.* **1991**, *54*, 525. (b) Reisfeld, R.; Jorgensen, J. K. *Struct. Bonding* **1992**, *77*, 207. (c) Castellano, F. N.; Meyer, G. J. *Prog. Inorg. Chem.* **1997**, *44*, 167.
(5) Meyer, T. J. *Acc. Chem. Res* **1989**, *22*, 364.
(6) O'Regan, B.; Grätzel, M. *Nature* **1991,** *353*, 737.
(7) (a) Anderson, S.; Constable, E. C.; Dare-Edwards, M. P.; Goodenough, J. B.; Hamnett, A.; Seddon, K. R.; Wright, R. D. *Nature* **1979**, *280*, 571. (b) Goodenough, J. B.; Dare-Edwards, M. P.; Campet, G.; Hamnett, A.; Wright, R. D. *Surf. Sci.* **1980**, *101*, 531. (c) Dare-Edwards, M. P.; Goodenough, J. B.; Hamnett, A.; Seddon, K. R.; Wright, R. D. *Faraday Discuss. Chem. Soc.* **1980**, *70*, 285.
(8) (a) Gerischer, H.; Michel-Beyerle, M. E.; Rebentrost, F.; Tributsch, H. *Electrochim. Acta* **1968**, *13*, 1509. (b) Tributsch, H. *Ber. Bunsen.-Ges. Phys. Chem.* **1969**, *73*, 582. (c) Gerischer, H.; Willig, F. *Top. Curr. Chem.* **1976**, *61*, 31. (d) Clark, W. D. K.; Sutin, N. *J. Am. Chem. Soc.* **1977**, *99*, 4676. (e) Spitler, M. T.; Calvin, M. *J. Chem. Phys.* **1977**, *66*, 4294. (f) Miyasaka, T.; Watanbe, T.; Fujishima, A.; Honda, K. *J. Am. Chem. Soc.* **1978**, *100*, 6657. (g) Miyasaka, T.; Watanbe, T.; Fujishima, A.; Honda, K. *Nature* **1979**, *277*, 638. (h) Shepard, V. R., Jr.; Armstrong, N. R. *J. Phys. Chem.* **1979**, *83*, 1268. (i) Jaeger, C. D.; Fan, F. F.; Bard, A. J. *J. Am. Chem. Soc.* **1980**, *102*, 2592. (j) Ghosh, P. K.; Spiro, T. G. *J. Am. Chem. Soc.* **1980**, *102*, 5543. (k) Kirsch-De Mesmaeker, A.; Dewitt, R. *Electrochim. Acta* **1981**, *26*, 297. (l) Daifuku, H.; Aoki, K.; Tokuda, K.; Matsuda, H. *J. Electroanal. Chem.* **1982**, *140*, 179. (m) Memming, R. *Prog. Surf. Sci.* **1983**, *17*, 7 and references therein.
(9) (a) Fujihara, M.; Ohishi, N.; Osa, T. *Nature* **1977**, *268*, 226. (b) Fujihara, M.; Kubota, M.; Osa, T. *J. Electroanal. Chem.* **1981**, *81*, 379.
(10) (a) Gerischer, H. *Photochem. Photobiol.* **1972**, *16*, 243. (b) Gerischer, H. *Electrochim. Acta* **1990**, *35*, 1677, and references therein.
(11) Meyer, G. J.; Searson, P. C. *Interface* **1993**, *2*, 23.
(12) Livage, J.; Henry, M.; Sanchez, C. *Prog. Solid State Chem.* **1988**, *18*, 259.
(13) (a) Moser, J.; Grätzel, M. *Helv. Chim. Acta* **1982,** *65*, 1436. (b) Moser, J.; Grätzel, M. *J. Am. Chem. Soc.* **1983**, *105*, 6547.
(14) Micic, O. I.; Zhang, Y.; Cromack, K. R.; Trifunac, A. D.; Thurnauer, M. C. *J. Phys. Chem.* **1993,** *97*, 7277.
(15) Nazeeruddin, M. K.; Liska, P.; Moser, J.; Vlachopoulos, N.; Grätzel, M. *Helv. Chim. Acta* **1990,** *73*, 1788.
(16) (a) Fox, M. A.; Lindig, B.; Chen, C.-C. *J. Am. Chem. Soc.* **1982**, *104*, 4, 5828. (b) Kamat, P. V.; Fox, M. A. *Chem. Phys. Lett.* **1983,** *102*, 379.
(17) Spanhel, L.; Anderson, M. A. *J. Am. Chem. Soc.* **1991**, *113*, 2826.
(18) Personal communication, Johnson Matthey Corp.
(19) (a) Desilvestro, J.; Gratzel, M.; Kavan, L.; Moser, J.; Augustynski, J. *J. Am. Chem. Soc.* **1985**, *107*, 2988. (b) Vlachopoulos, N.; Liska, P.; Augustynski, J.; Grätzel, M. *J. Am. Chem. Soc.* **1988**, *110*, 1216.
(20) Ettlinger, M. Technical Bulletin Pigments, No. 56, Degussa AG.
(21) Heimer, T. A.; D'Arcangelis, S. T.; Farzad, F.; Stipkala, J. M.; Meyer, G. J. *Inorg. Chem.* **1996**, *35*, 5319.
(22) Shklover, V.; Nazeeruddin, M.-K.; Zakeeruddin, S. M.; Barbé, C.; Kay, A.; Haibach, T.; Steurer, W.; Hermann, R.; Nissen, H.-U.; Grätzel, M. *Chem. Mater.* **1997**, *9*, 430.
(23) Hagfeldt, A.; Grätzel, M. *Chem. Rev. (Washington, D.C.)* **1995**, *95*, 49.
(24) Argazzi, R.; Bignozzi, C. A.; Heimer, T. A.; Castellano, F. N.; Meyer, G. J. *Inorg. Chem.* **1994**, *33*, 5741.
(25) Falaras, P.; Grätzel, M.; Hugot-Le Goff, A.; Nazeeruddin, M.; Vrachnou, E. *J. Electrochem. Soc.* **1993**, *140*, L92.
(26) Péchy, P.; Rotzinger, F. P.; Nazeeruddin, M. K.; Kohle, O.; Zakeeruddin, S. M.; Humphry-Baker, R.; Grätzel, M. *J. Chem. Soc., Chem. Commun.* **1995**, 65.
(27) (a) Liu, D.; Fessenden, R. W.; Hug, G. L.; Kamat, P. V. *J. Phys. Chem. B* **1997**, *101*, *2583*. (b) Hotchandani, S.; Bedja, I.; Fessenden, R. W.; Kamat, P. V. *Langmuir* **1994**, *10*, 17. (c) Bedja, I.; Hotchandani, S.; Kamat, P. V. *J. Phys. Chem.* **1993**, *97*, 11064. (d) Hotchandani, S.; Kamat, P. V. *Chem. Phys. Lett.* **1992**, *191*, 320. (e) Kamat, P. V.; Bedja, I.; Hotchandani, S.; Patterson, L. K. *J. Phys. Chem.* **1996**, *100*, 4900.
(28) (a) Juris, A.; Barigelletti, F.; Campagna, S.; Balzani, V.; Besler, P.; Von Zelewsky, A.*Coord. Chem. Rev.* **1988**, *84*, 85. (b) Meyer, T. J. *Acc. Chem. Res* **1989**, *22*, 364. (c) DeArmond, M. K.; Myrick, M. L. *Acc. Chem. Res* **1989**, *22*, 364. (d) Yersin, H.; Braun, D.; Hensler, G.; Gallhuber, E. In *Vibronic Processes in Inorganic Chemistry*; Flint, C. D., Ed.; Kluwer Academic Publishers: Dordrecht, 1989; p 195. (e) Balzani, V.; Scandola, F. *Supramolecular Photochemistry*; Ellis Harwood: Chichester, UK, 1990. (f) Kalyanasundaram, K. *Photochemistry of Polypyridine and Porphyrin Complexes*; Academic Press: New York, 1992; p 87.
(29) (a) Duonghong, D.; Borgarello, E.; Grätzel, M. *J. Am. Chem. Soc.* **1981**, *103*, 4685. (b) Humphry-Baker, R.; Lilie, J.; Grätzel, M. *J. Am. Chem. Soc.* **1982**, *104*, 422. (c) Duonghong, D.; Serpone, N.; Grätzel, M. *Helv. Chim. Acta* **1984**, *67*, 1012.
(30) O'Regan, B.; Moser, J.; Anderson, M.; Grätzel, M. *J. Phys. Chem.* **1990**, *94*, 8720.
(31) Kamat, P. V.; Bedja, I.; Hotchandani, S.; Patterson, L. K. *J. Phys. Chem.* **1994**, *98*, 4133.
(32) Cao, F.; Oskam, G.; Searson, P. C.; Stipkala, J. M.; Heimer, T. A.; Farzad, F.; Meyer, G. J. *J. Phys. Chem.* **1995**, *99*, 11974.
(33) (a) Kamat, P. V. *Prog. Inorg. Chem.* **1997**, *44*, 273. (b) Henglein, A. *Chem. Rev. (Washington, D.C.)* **1989**, *89*, 1861. (c) Matijevic, E. *Langmuir* **1986**, *2*, 12. (d) Ramsden, J. J. *Proc. R. Soc. London, Ser. A.* **1987**, *410*, 89. (e) Weller, H. *Adv. Mater.* **1993**, *5*, 88.
(34) (a) Fox, M. A.; Nobs, F. J.; Voynick, T. A. *J. Am. Chem. Soc.* **1980**, *102*, 4029. (b) Fox, M. A.; Nobs, F. J.; Voynick, T. A. *J. Am. Chem. Soc.* **1980**, *102*, 4036. (c) Dabestani, R.; Bard, A. J.; Campion, A.; Fox, M. A.; Mallouk, T. E.; Webber, S. E.; White, J. M. *J. Phys. Chem.* **1988**, *92*, 1872.
(35) (a) Kamat, P. V. *J. Phys. Chem.* **1989**, *93*, 859. (b) Kamat, P. V. *Langmuir* **1990**, *6*, 512. (c) Kamat, P. V.; Patrick, B. In *Electrochemistry in Colloids and Dispersions* Mackay, R. A., Texter, J., Eds.; VCH Publishers: New York, 1992; p 447. (d) Patrick, B.; Kamat, P. V. *J. Phys. Chem.* **1992**, *96*, 1423.
(36) (a) Moser, J.; Grätzel. M; Sharma, D. K.; Serpone, N. *Helv. Chim. Acta* **1985**, *68*, 1686. (b) Moser, J. E.; Grätzel, M. *Chem. Phys.* **1993**, *176*, 493.
(37) Rossetti, R.; Brus, L. E. *J. Am. Chem. Soc.* **1984**, *106*, 4336.
(38) Argazzi, R.; Bignozzi, C. A.; Heimer, T. A.; Castellano, F. N.; Meyer, G. J. *J. Phys. Chem. B* **1997,** *101*, 2591.
(39) (a) Ford, W. E.; Rodgers, M. A. J. *J. Phys. Chem.* **1994**, *98*, 3822. (b) Ford, W. E.; Rodgers, M. A. J. *J. Phys. Chem.* **1995**, *99*, 5139. (c) Ford, W. E.; Rodgers, M. A. J. *J. Phys. Chem.* **1995**, *99*, 7416. (d) Ford, W. E.; Rodgers, M. A. J. *J. Phys. Chem. B* **1997**, *101*, 930.
(40) Mulvaney, P.; Grieser, F.; Meisel, D. *Langmuir* **1990**, *6*, 567.
(41) Kim, Y. I.; Keller, S. W.; Krueger, J. S.; Yonemoto, E. H.; Saupe, G. B.; Mallouk, T. E. *J. Phys. Chem. B* **1997**, *101*, 2491.
(42) Heimer, T. A.; Meyer, G. J. *J. Lumin.* **1996**, *70*, 468.
(43) (a) James, D. R.; Ware, W. R. *Chem. Phys. Lett.* **1986**, *126*, 7. (b) Siemiarczuk, A.; Wagner, B. D. *J. Phys. Chem.* **1990**, *94*, 1661. (c) Ware, C. R. In *Photochemistry in Organized and Constrained Media* Ramurthy, V., Ed.; VCH Publishers: New York, 1991; Chapter 13
(44) (a) Albery, W. J.; Bartlett, P. N.; Wilde, C. P.; Darwent, J. R. *J. Am. Chem. Soc.* **1985**, *107*, 1854. (b) Kohlrausch, R. *Annalen* **1847**, *5*, 430. (c) Williams, G.; Watts, D. C. *Trans. Faraday Soc.* **1971**, *66*, 80.
(45) (a) Livesey, A. K.; Skilling, J. *Acta Crystallogr.* **1985**, *A41*, 113. (b) Livesey, A. K.; Licinio, P.; Delaye, M. *J. Chem. Phys.* **1986**, *84*, 5106. (c) Livesey, A. K.; Brochon, J. C. *Biophys. J.* **1987**, *52*, 693. (d) Brochon, J. C.; Livesey, A. K.; Pouget, J.; Valeur, B. *Chem. Phys. Lett.* **1990**, *174*, 517.
(46) Fessenden, R. W.; Kamat, P. V. *J. Phys. Chem.* **1995**, *99*, 12902.
(47) Sakata, T.; Hashimoto, K.; Hiramoto, M. *J. Phys. Chem.* **1990**, *94*, 4, 3040.
(48) Tachibana, Y.; Moser, J. E.; Grätzel, M.; Klug, D. R.; Durrant, J. *J. Phys. Chem.* **1996**, *100*, 20056.
(49) Gulino, D. A.; Drickamer, H. G. *J. Phys. Chem.* **1984**, *88*, 1173.
(50) Damrauer, N. H.; Cerullo, G.; Yeh, A.; Boussie, T. R.; Shank, C. V.; McCusker, J. K. *Science* **1997**, *275*, 54.
(51) Argazzi, R.; Bignozzi, C. A.; Heimer, T. A.; Meyer, G. J. *Inorg. Chem.* **1997**, *36*, 2.
(52) Nazeerudin, M. K.; Kay, A.; Rodicio, I.; Humphrey-Baker, R.; Müller, E.; Liska, P.; Vlachopoulos, N.; Gratzel, M. *J. Am. Chem. Soc.* **1993**, *115*, 63820.
(53) Nazeeruddin, M. K.; Liska, P.; Moser, J.; Vlachopoulos, N.; Grätzel, M. *Helv. Chim. Acta* **1990**, *73*, 1788.
(54) (a) Kay, A.; Grätzel, M. *J. Phys. Chem.* **1993**, *97*, 6272. (b) Kay, A.; Humphry-Baker, R.; Grätzel, M. *J. Phys. Chem.* **1994**, *98*, 952.

(55) (a) Gopidas, K. R.; Kamat, P. V. *J. Phys. Chem.* **1989**, *93*, 6428. (b) Kamat, P. V. *Prog. Reaction Kinetics* **1994**, *19*, 277 and references therein. (c) Nasr, C.; Liu, D.; Hotchandani, S.; Kamat, P. V. *J. Phys. Chem.* **1996**, *100*, 11054.
(56) Lu, H.; Prieskorn, J. N.; Hupp, J. T. *J. Am. Chem. Soc.* **1993**, *115*, 4927.
(57) Willig, F.; Eichberger, R.; Sundaresan, N. S.; Parkinson, B. A. *J. Am. Chem. Soc.* **1990**, *112*, 2702.
(58) (a) Albery, W. J.; Bartlett, P. N.; Porter, J. D. *J. Electrochem. Soc.* **1984**, *131*, 2892. (b) Albery, W. J.; Bartlett, P. N. *J. Electrochem. Soc.* **1984**, *131*, 315. (c) Rothenberger, G.; Fitzmaurice, D.; Grätzel, M. *J. Phys. Chem.* **1992**, *96*, 5983.
(59) Heimer, T. A.; Bignozzi, C. A.; Meyer, G. J. *J. Phys. Chem.* **1993**, *97*, 11987.
(60) Yan, S. G.; Hupp, J. T. *J. Phys. Chem.* **1996**, *100*, 6867.
(61) Zaban, A.; Ferrere, S.; Sprague, J.; Gregg, B. A. *J. Phys. Chem. B* **1997,** *101*, 55.
(62) Argazzi, R.; Bignozzi, C. A.; Heimer, T. A.; Castellano, F. N.; Meyer, G. J. *J. Am. Chem. Soc.* **1995**, *117*, 11815.
(63) Fitzmaurice, D.; Frei, H. *Langmuir* **1991**, *7*, 1129.
(64) (a) Heimer, T. A.; Meyer, G. J. *Proc. Electrochem. Soc.* **1994**, *95*−*98*, 167. (b) Heimer, T. A. Ph.D. Thesis, Johns Hopkins University, 1996.
(65) Fahrenbruch, A. L.; Bube, R. H. *Fundamentals of Solar Cells Photovoltaic Solar Energy Conversion*, Academic Press: New York, 1983.
(66) (a) Nazeeruddin, M. K.; Kay, A.; Rodicio, I.; Humphry-Baker, R.; Muller, E.; Liska, P.; Vlachopoulos, N.; Gratzel, M. *J. Am. Chem. Soc.* **1993**, *115*, 6382. (b) Lindstrom, H.; Rensmo, H.; Sodergren, S.; Solbrand, A.; Lindquist, S. E. *J. Phys. Chem.* **1996**, *100*, 3084. (c) Huang, S. Y.; Schlichthorl, G.; Nozik, A. J.; Grätzel, M.; Frank, A. J. *J. Phys. Chem. B* **1997**, *101*, 2576.
(67) Tan, M. X.; Laibinis, P. E.; Nguyen, S. T.; Kesselman, J. M.; Stanton, C. E.; Lewis, N. S. *Prog. Inorg. Chem.* **1994**, *41*, 21 and references therein.
(68) Bonhote, P.; Grätzel, M.; Jirousek, M.; Liska, P.; Pappas, N.; Vlachopoulos, N.; von Plata, C.; Walder, L. *Tenth International Conference on Photochemical Conversion and Storage of Solar Energy*, 1994; Abstract C2.
(69) (a) Kalyanasundaram, K.; Vlachopoulos, N.; Krishnan, V.; Monnier, A.; Grätzel, M. *J. Phys. Chem.* **1987**, *91*, 2342. (b) Enea, O.; Moser, J.; Grätzel, M. *J. Electroanal. Chem.* **1989**, *259*, 59.
(70) Kittel, C. In *Introduction to Solid State Physics*; John Wiley & Sons: New York, 1977.
(71) (a) Konenkamp, R.; Henninger, R.; Hoyer, P. *J. Phys. Chem.* **1993**, *97*, 7328. (b) Sodergren, S.; Hagfeldt, A.; Olsson, J.; Lindquist, S.-E. *J. Phys. Chem.* **1994**, *98*, 5552. (c) Vinodgopal, K.; Hua, X.; Dahlgren, R. L.; Lappin, A. G.; Patterson, L. K.; Kamat, P. V. *J. Phys. Chem.* **1995**, *99*, 10883. (d) Cao, F.; Oskam, G.; Searson, P. C.; Meyer, G. J. *J. Phys. Chem.* **1996**, *100*, 17021.
(72) (a) Augustynski, J. *Struct. Bonding* **1988**, *69*, 1. (b) Finklea, H. O. In *Semiconductor Electrodes;* Finklea, H. O., Ed.; Elsevier: Amsterdam, 1988.
(73) (a) Ocana, M.; Hsu, W. P.; Matijevic, E. *Langmuir* **1991**, *7*, 2911. (b) Haus, J. W.; Zhou, H. S.; Honma, I.; Komiyama, H. *Phys. Rev. B* **1993**, *47*, 1359.
(74) Bedja, I.; Kamat, P. V. *J. Phys. Chem.* **1995**, *99*, 9182.
(75) (a) Liu, C.; Pan, H. P.; Fox. M. A.; Bard, A. J. *Science* **1993**, *261*, 897. (b) Debreczeny, M. P.; Svec, W. A.; Marsh, E. M.; Wasielewski, M. R. *J. Am. Chem. Soc.* **1996**, *118*, 8174.
(76) Bechinger, C.; Ferrere, S.; Zaban, A.; Sprague, J.; Gregg, B. A. *Nature* **1996**, *383*, 608.
(77) Athanassov, Y.; Rotzinger, F. P.; Pecy, P.; Grätzel, M. *J. Phys. Chem. B.* **1997**, *101*, 2558.

CM9703177